Supplementary Info

Estimation of the spontaneous mutation rate by short term mutation accumulation lines in the non-biting midge *Chironomus riparius*

Ann-Marie Oppold & Markus Pfenninger

Figure S1. Scheme of the experimental design.

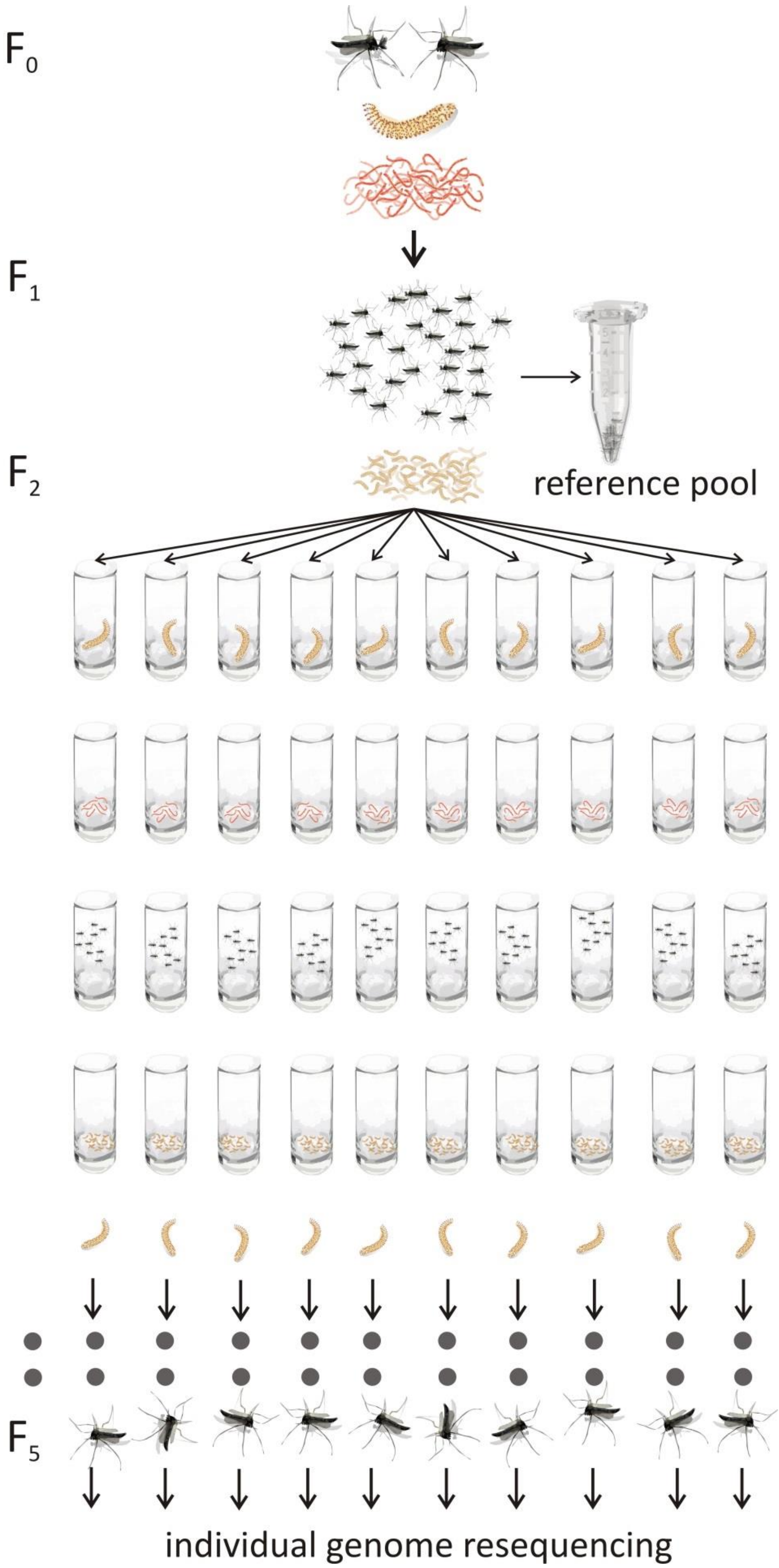

Table S2. Derivation of probabilities to observe a mutation in either heterozygous or homozygous state, depending on the generation of their occurrence.

1 = mutant allele 0 = ancestral allele		mutant allele frequency						p mutant allele heterozygous	p mutant allele homozygous
F1		1 individual						**1.00**	**0.00**
possible genotype combinations to produce the next generation		10|00							
probability of occurrence		1.000							
resulting mutant allele frequency in the offspring		0.250							
F2								**1.00**	**0.00**
	11	0.000							
	10	0.500							
	00	0.500							
possible genotype combinations to produce the next generation		10|10	10|00	00|00					
probability of occurrence		0.250	0.500	0.250					
resulting possible mutant allele frequency in the offspring		0.500	0.250	0.000					
F3									
resulting genotype frequencies									
	11	0.250	0.125	0.000					
	10	0.500	0.375	0.000					
	00	0.250	0.500	1.000					
overall probability (= prob of occurrence * allelefrequency)									
	11	0.063	0.031	0.000				**0.77**	**0.23**
	10	0.125	0.188	0.000					
	00	0.063	0.281	0.250					
possible genotype combinations to produce the next generation		11|11	11|10	10|10	11|00	10|00	00|00		
probability of occurrence		0.023	0.109	0.133	0.109	0.250	0.391		
resulting mutant allele frequency in the offspring		1.000	0.750	0.500	0.500	0.250	0.000		
F4									
resulting genotype frequencies									
	11	1.000	0.563	0.250	0.250	0.063	0.000		
	10	0.000	0.375	0.500	0.500	0.375	0.000		
	00	0.000	0.063	0.250	0.250	0.563	1.000		
overall genotype probability									
	11	0.023	0.062	0.033	0.027	0.016	0.000	**0.61**	**0.39**
	10	0.000	0.041	0.066	0.055	0.094	0.000		
	00	0.000	0.007	0.033	0.027	0.141	0.391		
possible genotype combinations to produce the next generation		11|11	11|10	10|10	11|00	10|00	00|00		
probability of occurrence		0.074	0.118	0.111	0.056	0.171	0.485		
resulting mutant allele frequency in the offspring		1.000	0.750	0.500	0.500	0.250	0.000		
F5									
resulting genotype frequencies									
	11	1.000	0.563	0.250	0.250	0.063	0.000		
	10	0.000	0.375	0.500	0.500	0.375	0.000		
	00	0.000	0.063	0.250	0.250	0.563	1.000		
overall probability									
	11	0.074	0.067	0.028	0.014	0.011	0.000	**0.50**	**0.50**
	10	0.000	0.044	0.056	0.028	0.064	0.000		
	00	0.000	0.007	0.028	0.014	0.096	0.485		
possible genotype combinations to produce the next generation		11|11	11|10	10|10	11|00	10|00	00|00		
probability of occurrence		0.123	0.100	0.082	0.041	0.119	0.550		

Table S1. List of identified mutations. Given are the mutation accumulation line (Ma) in which theiy were identified, the scaffold and base pair position, the mutation type, the sequence context 10 bp up- and downstream, the base in the reference pool, the mutated base, whether the mutation is a transistion (TS) or transversion (TV), mutation from A/T to G/C or vice versa, indication whether mutation confirmation was attempted via Sanger sequencing and whether the mutation could be confirmed and if so, if it occurred in heterozygous (hetero) and/or homozygous (homo) state.

Ma line	scaffold	position	mutation type	context	reference base	mutation	TS/TV	gene	A/T> C/G	C/G> A/T	Sanger checked	confirmed	allelic state
A1	scaffold1	1408155	insertion	ATTTATAGTA**T**TTTTTAACTT	A	AT					yes	yes	hetero
	scaffold31	219294	SNP	TTTTACATCC**C**AGACGAATTT	G	C	TV				yes	yes	homo
	scaffold45	344749	SNP	GCTTGTGGTT**A**ACACAGTCAG	G	A	TS			+	yes	yes	homo/hetero
	scaffold150	125441	insertion	TTGATTTTTG**A**AAAAAAGCGA	G	GA					yes	yes	hetero
	scaffold200	81719	insertion	AATGATAAAG**A**AATGTATCAA	G	GA					yes	no	hetero
	scaffold270	8038	deletion	TAAGTTCCTA-TTTTTTTTTA	AT	A		yes			yes	yes	hetero
	scaffold283	32972	deletion	TCAATTCACC-AAAAAAATGA	CA	C							
A2	scaffold25	413316	SNP	CTCAGAATTG**T**ATAGATGATG	C	T	TS			+	yes	yes	hetero
	scaffold31	1191434	SNP	GAAAAAAAGA**A**ATTCAAATAG	G	A	TS			+	yes	yes	hetero
	scaffold69	447444	insertion	CCAAATCATG**T**TTTTTTTTTG	G	GT					yes	yes	hetero
	scaffold412	200133	deletion	GCAGCATACC-AAAAAAAATC	CA	C					yes	yes	hetero
A3	scaffold7	509054	deletion	ACAAAATCCA-TTTTTTTTTA	AT	A					yes	yes	hetero
	scaffold40	219059	deletion	CGTTGATTGC-AAAAAAAATG	CA	C					yes	yes	hetero
	scaffold623	9623	SNP	TTCGAAAGAG**A**ACAAATTAAA	G	A	TS			+			
A4	scaffold5	386370	insertion	AATTTATAAC**A**AAAAAAATTA	C	CA					yes	no	hetero
	scaffold26	201140	insertion	TACAAGAAAC**A**AAAAAAAAAA	C	CA					yes	yes	homo
	scaffold50	791827	SNP	TAGTCGTAAG**T**TAGAAAATTA	G	T	TV			+	yes	yes	hetero
	scaffold154	181197	SNP	TACAAATATT**T**ACTCACGAAG	G	T	TV			+	yes	yes	hetero

	scaffold163	312123	SNP	ATTATTACGG**C**CTCCATGCAA	T	C	TS	+		yes	yes	hetero
	scaffold167	76594	deletion	CAGTTTTTTC**-**AAAAAAAATT	CA	C				yes	yes	hetero
	scaffold985	8371	SNP	ACAAATTCAC**G**TGGCTCCAGG	A	G	TS	+				
A5	scaffold17	651170	SNP	TAAAGGCAAA**C**CCAAAAAAAA	A	C	TV	+		yes	yes	homo/hetero
	scaffold29	336162	insertion	TGTCAAAACA**T**TTTTTTTTTT	A	AT						
	scaffold59	149577	SNP	TAGGGTTGAT**T**CCATCAAATT	A	T	TV					
	scaffold121	54814	deletion	ATTATTTAAT**-**GATGTTACGC	TG	T				yes	no	hetero
	scaffold189	137440	deletion	ACAAGATCAA**-**TTTACATACG	AT	A						
	scaffold195	134136	insertion	TCCATAAAAG**C**CCCCCCCCCC	G	GC						
	scaffold267	22672	SNP	GTAAGTCTGT**A**CATTCTTCTC	C	A	TV		+	yes	yes	homo
	scaffold276	23996	SNP	GAGATCTGGA**C**CTACTCTAAG	G	C	TV			yes	yes	homo/hetero
	scaffold326	93251	deletion	GAATCATTCG**-**CCAAACCTTG	GC	G						
A6	scaffold243	29748	SNP	CTCTAGGTCC**T**TTCCATTAAA	G	T	TV		+	yes	yes	hetero
	scaffold256	114637	SNP	ATTCCATTCG**T**GTTGAGGAAT	A	T	TV			yes	yes	hetero
	scaffold382	67246	deletion	CTGTAAATAA**-**TTTTTTTTTG	AT	A				yes	no	hetero
	scaffold581	46883	deletion	TAACTTAAGA**-**TTTTTTTTTT	AT	A				yes	yes	hetero
A7	scaffold185	145141	SNP	AAAACAGCCG**A**GAACTAGCGG	G	A	TS		+			
	scaffold282	7409	deletion	TTTCAAGAAC**-**TTTTTTTGCA	CT	C				yes	yes	hetero
	scaffold637	12063	deletion	GGGTTTACCA**-**TTTTTTTTGG	AT	A				yes	yes	hetero
A8	scaffold5	658683	deletion	GCATTTTGAC**-**AAAAAAAAAT	CA	C						
	scaffold26	630176	SNP	ATTACAAAAA**A**AAATTCGCAG	T	A	TV			yes	no	hetero
	scaffold49	749494	SNP	ATTACAAAAA**A**AAATTCGCAG	A	C	TV	+		yes	yes	hetero

	scaffold75	243457	deletion	ACTTCCATCA-TTTTTTTTTG	AT	A				yes	yes	hetero
	scaffold189	289120	SNP	CAATTGTTGA**C**GGATCTTATA	T	C	TS	+		yes	no	hetero
	scaffold454	67203	deletion	AGAAAAAAAG-TTTTTTTTGT	GT	G				yes	yes	hetero
	scaffold721	3700	SNP	GATCCATCAA**T**ATTGTCTGTT	C	T	TS		+			
A9	scaffold935	4628	deletion	TAATAGTTTG-AAAAAAAAAT	GA	G						
	scaffold1577	4603	SNP	GTATTTTTCA**G**CAGTTCAAAA	A	G	TS	+		yes	yes	hetero
	scaffold1577	4957	SNP	CATCTATCCA**T**TCTGTCATTA	C	T	TS		+			
A10	scaffold8	773458	SNP	AACAACAGCT**A**AGTCAATGCA	G	A	TS		+	yes	yes	homo/hetero
	scaffold32	504864	SNP	CGTGTCTGTA**G**GGACGTGTCT	A	G	TS	+		yes	yes	homo/hetero
	scaffold146	343308	SNP	ATGTAACACA**T**TGTACAGTTA	C	T	TS		+	yes	yes	hetero
	scaffold304	122155	SNP	ATCAATAGCT**A**CACATCAGCT	C	T	TS		+			

Text S1

Supplemental Text 1

Influence of genomic base composition on mutation targets in *C. riparius*

Even though the overall single base mutation rate of *C. riparius* was very similar to those published for other insects (e.g. (Keightley *et al.* 2014; Keightley *et al.* 2009), the mutational spectrum found here was strongly shifted from SPM to indel mutations. The latter occurred preferentially in A/T monomer nucleotide runs (21 out of 25). After Sanger sequencing confirmation that this is not due to mapping or assembly artefacts, the bias raised the suspicion that perhaps the high genomic AT content could be responsible for this pattern, moreover since such a bias could also affect the abundance of CpG motives, known for their susceptibility to point mutations (Bird 1980).

To infer potential causes for this shift in the mutational spectrum in *C. riparius*, we first explored the effect of base composition bias on the expected abundance, length and nucleotide bias of monomer runs and CpG motives. We simulated 1000 DNA stretches of 1 Mb length by randomly drawing bases from different base compositions (50%, 60%, 70% and 80% AT content). We then recorded the frequency length distribution of resulting monomer stretches longer than 5 bp and CpG motives of all length.

Both the expected mean number and mean length of all monomer runs increased with increasing base composition bias (Figure 1, left), comprising between 1.6% of all base positions for 50% AT content and 6.9% for 80% AT content. The ratio of A/T vs. G/C monomer runs increased exponentially from 1 (50% AT content) to 680 (80% AT content, Figure 1, right). As expected, the opposite was true for CpG motives that were more abundant and longer with lower AT content (Figure 1, right), comprising between 3.1 % (80% AT content) and 14.7% (50% AT content) of the positions. This showed that just for statistic reasons, the abundance, length distribution and bias in monomer and CpG runs depends strongly on the genomic base composition of the respective organism.

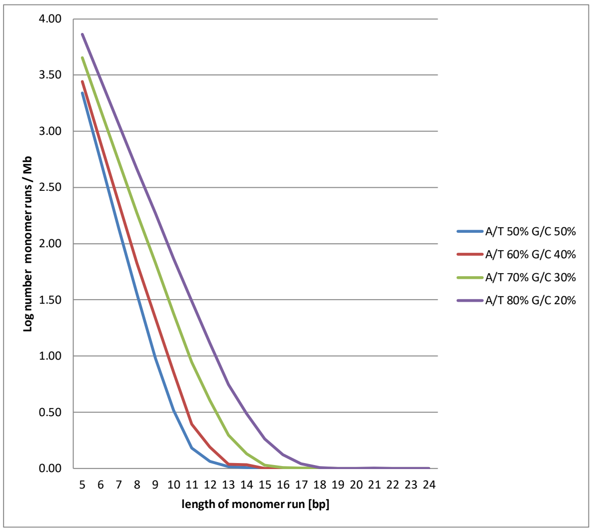

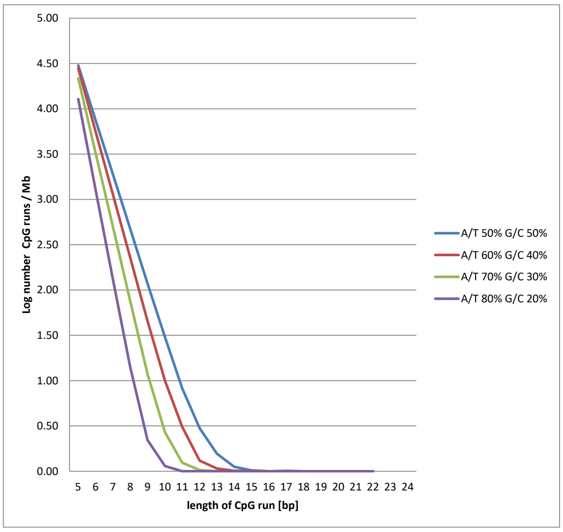

Figure 1. Influence of base composition bias on the expected abundance and length of monomer and CpG runs. Left) Logarithmic plot of mean expected monomer runs per Mb as a function of their length for different base compositions. Right) Logarithmic plot of mean expected CpG runs per Mb as a function of their length for different base compositions.

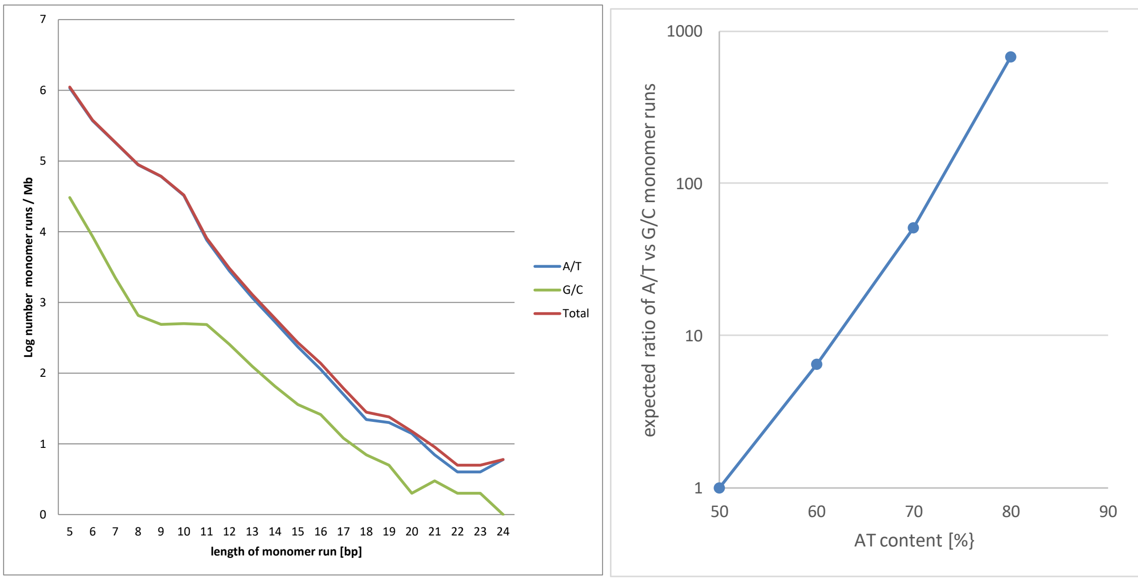

Figure 2. Left) Logarithmic plot of observed monomer runs frequencies for all (red), A/T (blue) and G/C (green) runs. Right) Expected ratio of A/T to G/C monomer runs as a function of the AT content.

We then counted the monomer runs between 5-24 bp in the reference genome of *C. riparius*. In total, there were more than 1.8 million of such monomer runs. The length distribution of the monomer runs was roughly exponentially declining (Figure 2).

The vast majority of them were A/T runs (1.82 million) versus only 43778 G/C runs (Table 1, ratio 41.6). This makes up 5.87% and 0.14% of the high complexity regions of the reference genome, respectively. In terms of base pair composition, the A/T content of the monomer runs (98%) exceeded by far the genome-wide average (69%, (Oppold *et al.* 2016)) and is thus contributing to the high A/T content of the *C. riparius* genome.

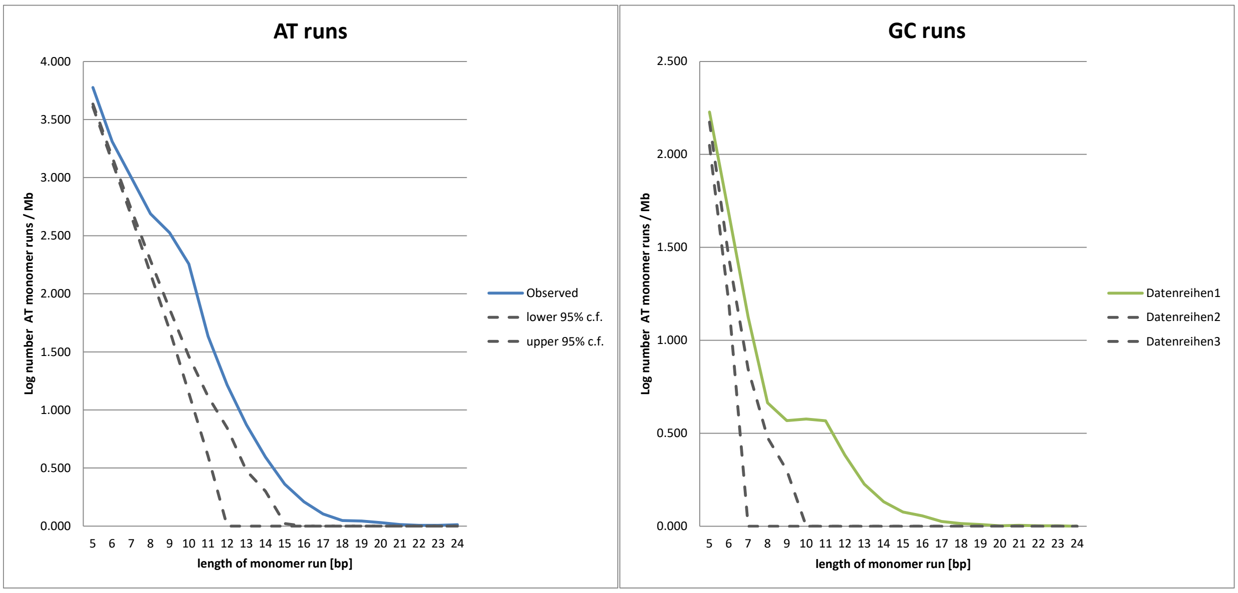

Figure 3. Logarithmic plot of expected (dashed lines, 95% confidence interval) and observed number of monomer runs per Mb (solid line) for left) A/T runs and right) G/C runs.

To infer whether monomer stretches are just random products of the general base pair composition of *C. riparius*, we simulated 1000 DNA stretches of 1 Mb each by randomly drawing from the

Table 1. Basic statistics of the monomer run content and CpG positions of the high complexity regions of the *C. riparius* reference genome.

	Total number	Base pairs	Proportion	Percent of the genome
A/T	1,824,305	10,606,267	0.977	5.87
G/C	43,778	245,544	0.023	0.14
All	1,868,083	10,851,811		6.01
CpG	4,259,457	9,828,478		5.44

observed base pair distribution in the genome (A 34.5%, T 34.5%, G 15.5%, C 15.5%) and calculated the 95% confidence interval for the occurrence of monomer runs from 5 – 24 base pairs. Normalising the observed number of monomer runs to 1 Mb for comparison showed that for both A/T and G/C runs, the observed number of monomer runs was greater than the expected. The difference was lower for shorter runs and increased for longer runs (Figure 3).

This suggested that not only random processes are responsible for the observed abundance and length distribution of monomer runs in the *C. riparius* genome. This interpretation is supported by the fact that indel mutations occurred significantly more often in monomer stretches longer than 5 bp than in the rest of the genome (21 versus 4 in 5.87% vs. 94.13% of the genome, respectively, X^2 = 345.1 $p < 0.0001$). In addition, the probability for an indel mutation (*i.e.* the mutation rate) strongly increased with the length of the stretch (Figure 4 (Bacon *et al.* 2001)).

Even though there were more deletions than insertions observed in monomer runs (14 : 7), this difference was not significant, based on a 1:1 expectation (X^2 = 2.33 p = 0.127). There was also no significant trend for insertions or deletions to occur preferentially in either short (< 9) or long (>= 9) monomer runs (Fisher's exact test p = 0.280). There was no significant difference in mutability of A/T versus G/C runs, taking their different abundance in the genome into account (21 and 1 mutations observed, expected frequencies 0.987 and 0.023, respectively, X^2 = 0.562 p = 0.453). However, despite the comparatively large number of mutations available for analysis in this study, these results may change with an increasing number of observed mutations.

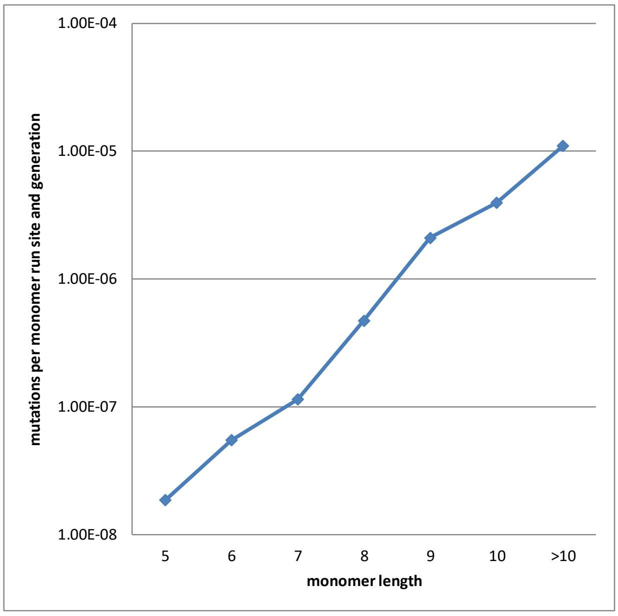

Figure 4. Estimated mutation rates for different monomer run lengths per run site and generation. Please note the logarithmic scale.

These findings suggested the following model: Short monomer runs occur by chance, respectively are an universal unavoidable effect of the limited number of different DNA bases. Above a certain length threshold, their further dynamic is driven by indel mutations to which these monomer runs are inherently increasingly susceptible with increasing length (Lai & Sun 2003). The more the genomic base composition deviates from uniformity, the more and the longer monomer runs the respective genome has and thus more indel mutations are expected. In addition, in case of an AT bias as observed here, the number of CpG sites decreases and thus the probability for point mutations which should shift the ratio even further in favour of indel mutations.

To test this prediction with empirical data, we compared the monomer and CpG run content among *C. riparius* and *D. melanogaster* (genome version 6.12 downloaded from flybase.org on 13.1.2017). The base pair composition of *D. melanogaster* was estimated from the data to 57.6% AT and 42.4% GC as opposed to 69.0% AT and 31.0% GC in *C. riparius*. In both species, the observed monomer run abundance and length was larger than expected from the base composition (Figure 5, left). However,

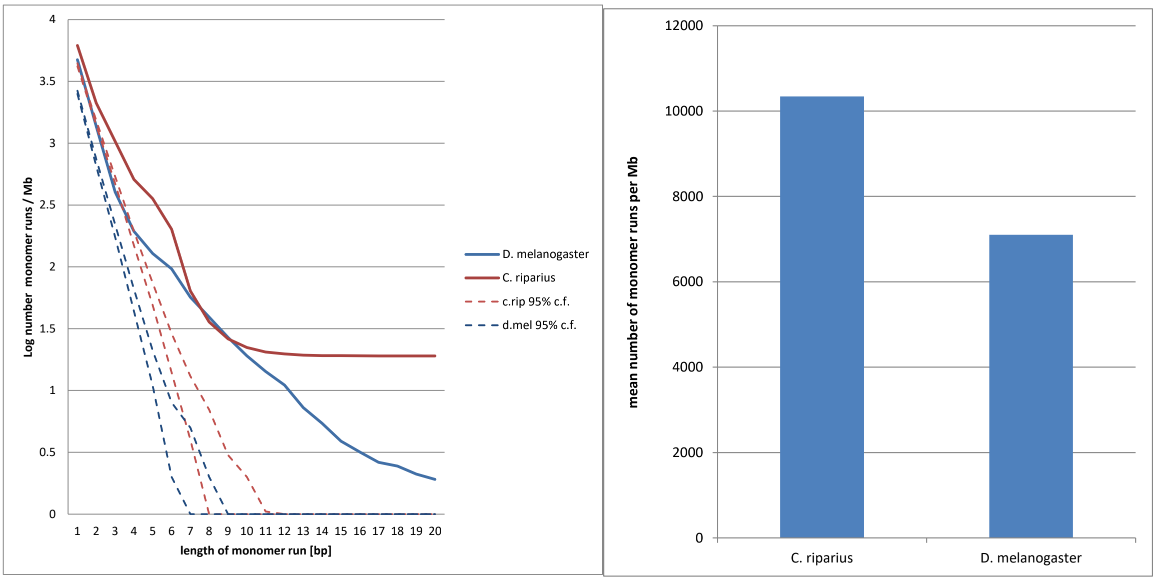

Figure 5. Comparison of genomic monomer runs content among *C. riparius* and *D. melanogaster*. left) Logarithmic plot of the observed (solid line) log number of monomer runs per 1 Mb as a function of their length with the 95% confidence interval as expected according to the genomic base pair composition. right) Mean number of monomer runs larger 5 bp per 1 Mb.

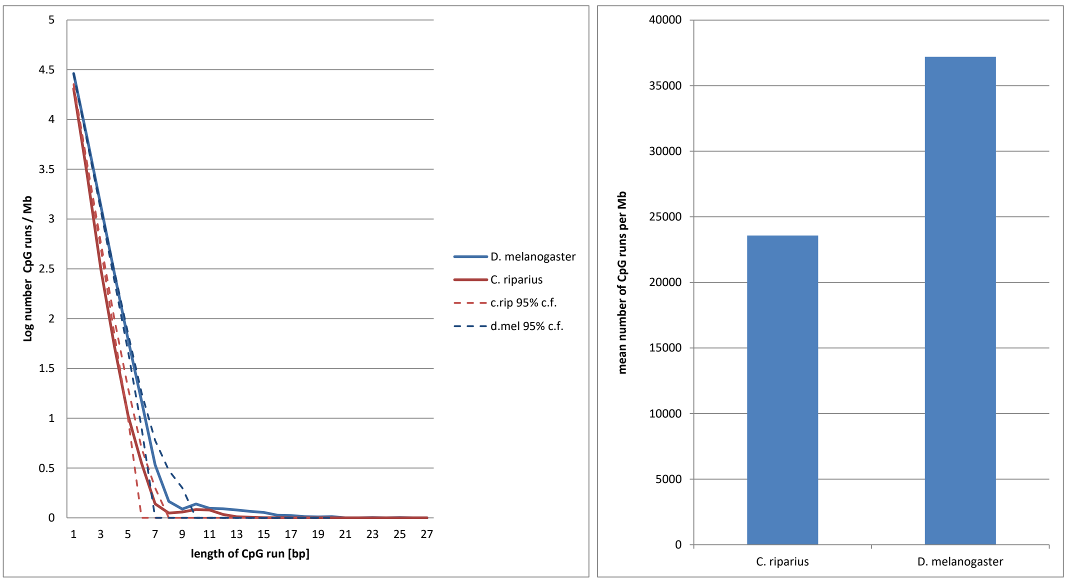

Figure 6. Comparison of genomic CpG runs content among *C. riparius* and *D. melanogaster*. left) Logarithmic plot of the observed (solid line) log number of CpG runs per 1 Mb as a function of their length with the 95% confidence interval as expected according to the genomic base pair composition. right) Mean number of CpG runs per 1 Mb.

apart from monomers of 9-11 bp length, there were consistently more repeats per Mb in *C. riparius*, which was mirrored in the much higher total abundance (Figure 5, right) and proportion of the genome (6.01% vs. 4.08%, respectively). Therefore, there are much more opportunities for indel mutations in monomer runs in the *C. riparius* genome compared to *D. melanogaster*. It would have been interesting to compare the indel mutation rates for different monomer run length classes, however, there is not enough data available for *D. melanogaster*.

In contrast, the content of CpG runs was mostly within the statistical expectations, except for the longest (and rarest) runs (Figure 6, left). In contrast to monomer runs, the picture was reversed, *D. melanogaster* harboured more CpG motives per Mb than *C. riparius*, according to the expectations from the respective genomic AT content (Figure 6, right). Both findings could explain the observed shift in mutational spectrum among the two species.

In conclusion, the observed accumulation of indel mutations in A/T mononucleotide runs and the relatively low ratio of SMP to indels in *C. riparius* is most probably due to the AT bias of the entire genome which increases both the relative and absolute number and length of potential indel mutation targets and simultaneously decreases the respective potentially particular susceptive CpG point mutation positions.

References

Oppold A-M, Schmidt H, Rose M*, et al.* (2016) *Chironomus riparius* (Diptera) genome sequencing reveals the impact of minisatellite transposable elements on population divergence. *bioRxiv*, 080721.

Keightley PD, Ness RW, Halligan DL, Haddrill PR (2014) Estimation of the Spontaneous Mutation Rate per Nucleotide Site in a *Drosophila melanogaster* Full-Sib Family. *Genetics* **196**, 313-320.

Keightley PD, Trivedi U, Thomson M*, et al.* (2009) Analysis of the genome sequences of three Drosophila melanogaster spontaneous mutation accumulation lines. *Genome Research*, gr. 091231.091109.

Lai Y, Sun F (2003) The relationship between microsatellite slippage mutation rate and the number of repeat units. *Molecular Biology and Evolution* **20**, 2123-2131.

Bacon AL, Dunlop MG, Farrington SM (2001) Hypermutability at a poly (A/T) tract in the human germline. *Nucleic Acids Research* **29**, 4405-4413.

Bird AP (1980) DNA methylation and the frequency of CpG in animal DNA. *Nucleic Acids Research* **8**, 1499-1504.